Automatic Lung Nodule Identification Using Bayesian Approach

[*]M.Mary Adline Priya, [#]Dr. S.Joseph Jawhar

[*]Research Scholar, [#]Professor, [*]Faculty of Information and Communication Engineering, [#]Faculty of Electrical and Electronics Engineering, Arunachala College of Engineering for Women, Kanya Kumari, India, [*]michaelpriya21@gmail.com

Abstract: Chest computed tomography (CT) images and their quantitative analyses have become increasingly important for a variety of purposes including lung parenchyma density analysis, airway analysis, diaphragm mechanics analysis, and nodule detection for cancer screening. Lung segmentation is an important prerequisite step for automatic image analysis. A novel lung segmentation method to minimize the juxta-pleural nodule is presented in this work, which is a notorious challenge in the applications.

***Index Terms*— Active Contour, Lung Segmentation, Chest CT images, Computer aided diagnosis, Juxta-pleural Nodule**

I. INTRODUCTION

Pulmonary or chest computed tomography (CT) images have been used for a variety of purposes, such as lung parenchyma density analysis [1, 2], airway analysis [3, 4], diaphragm mechanics analysis [5, 6] and nodule detection for cancer screening [7]. Recently, with the aid of computing technology, it has become feasible to conduct automatic quantitative analyses. In addition, collaboration among engineers, clinicians, and data scientists has led to the development of accurate automated screening programs for clinical use. Lung segmentation, a step required prior to chest CT imaging analysis, is a crucial starting point for all lung-related quantitative analysis.

II. PROPOSED WORK

The main contributions of this study are: We proposed a Bayesian approach for automatic juxta-pleural nodule identification in the lung segmentation stage from chest CT scans. We presented a concave point detection and circle/ellipse Hough transform to minimize false positives. We tested our proposed method from 16,873 images (84 subjects). Among the images, 314 images included juxta-plerual nodules.

We further validated the method from different databases, which included 1,766 images in total. Among the images, 125 included juxta-pleural nodules. We presented the extension capability that accurate lung contour segmentation results can be provided from any global contour results by applying to our proposed method framework.

A. Collection of input data:

For the clinical data, we collected chest CT digital imaging and communications in medicine (DICOM) images of 84 anonymous subjects, including 42 subjects with juxta-pleural nodules. Each scan included 150 to 215 image frames, and there were 16,873 images in total. Among the images, 314 included juxta-pleural nodules.

B. Global Lung Contour Extraction with the Chan-Vese model:

To segment the lung contour, we first applied the CV model to chest CT images. After applying with the CV model on the chest CT image, the nodules or vessels inside the lung parenchyma are also segmented. To separate them from the lung contour, we selected the two longest contours, which correspond to left and right lungs. Fig. 1 shows the CV model-based lung segmentation results from four chest CT images. For the CV model-based lung segmentation, we chose the generally used parameters of ν=0 and $\lambda 1$= $\lambda 2$=1. The parameter of μ=0.01 was chosen by providing the highest accuracy. As μ increases, the results tend to be roughly segmented. All of the parameters were applied to the entire images in this paper.

The CV model method provided mostly accurate lung wall segmentation results, as shown in Figs. 1(a) and (b). In particular, in Fig. 1(b), the juxta-pleural nodule is included within the segmented lung contour. On the other hand, in Fig. 1(c), the juxta-pleural nodule is outside the segmented lung contour. This is because the pixel intensities of the juxta-pleural nodule and the adjacent surrounding tissue nearly overlap. The juxta-pleural nodule outside the lung contour ultimately results in missed nodules and incorrect

 DOI : 10.35291/2454-9150.2019.0364

quantitative analyses. In the following subsections, we adopted a Bayesian approach to minimize this juxta-pleural nodule issue.

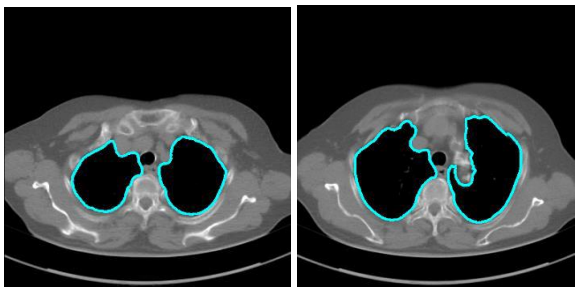

(a) (b)

(c)

Fig 1. Lung segmentation results using Chan–Vese (CV) model. (a) Most lung contours can be accurately segmented. (b) A correct segmentation results in the presence of a juxta-pleural nodule. (c) An incorrect segmentation results in the presence of a juxta-pleural nodule; the incorrect part is pointed by an arrow.

C. A Bayesian approach to juxta-pleural nodule candidate detection:

Given the N successive chest CT image frames, we denote the lung contour state vector of the n-th image by CFn (i.e. $CF1$, $CF2$, ... CFN). Note again that the frame represents the spatially sliced image from top to bottom. The state vector CFn is assumed to evolve according to the following system model as

$$C_F^n = f_n(C_F^{n-1}, w^n) \quad (1)$$

D. Elimination of false positives:

For classifying the nodule candidates as true nodules or false positives, we first investigated whether each candidate contour included any concave point from the center point of CGn. Let us denote the set of contour points of each nodule candidate by

$$\boldsymbol{P}_c^{n(i)} = \left\{ P_c^{n(i,j)} : j = 1,2,\dots J \text{ and } i = 1,2,\dots I \right\}, \quad (2)$$

E. Feature Extraction:

Features are extracted and passed to the selected classifier to help in raising the accuracy of classification. Different features are used including shape features, texture features, statistical features and intensity features.

III. PERFORMANCE MEASURES

The performance of our proposed method was evaluated using five metrics: the disc similarity coefficient (DSC), modified Hausdorff distance (MHD), sensitivity, specificity, and accuracy. To compute the five metrics, we first calculated the true positive (TP), false positive (FP), true negative (TN), and false negative (FN) values. TP (FP) is the number of positive pixels labelled correctly (incorrectly). TN (FN) is the number of negative pixels labeled correctly (incorrectly). We used an example to quantize the parameters in Fig. 2. In Fig. 2 (a), the gold standard contour (purple) and the estimated contour (blue) are shown, and the corresponding TP, FP, TN, and FN are shown in Fig 2(b). Each estimated contour was evaluated with each gold standard contour for all images.

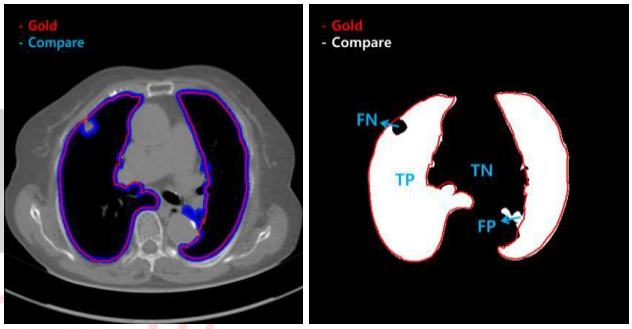

(a) *(b)*

Fig 2. (a) Example of the gold standard contour (purple) and estimated contour (blue), and (b) the corresponding true positive (TP), true negative (TN), false positive (FP), and false negative (FN).

Based on the four parameters, the DSC can be calculated as

$$DSC = 2TP/\ 2TP+FP+FN \quad (3)$$

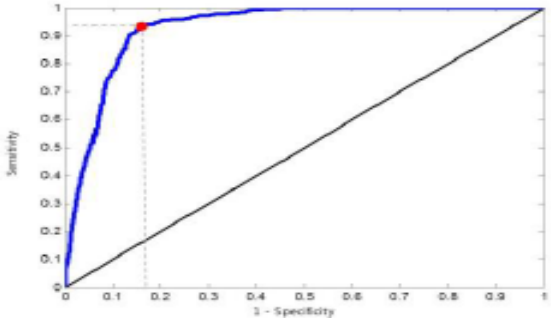

Fig 3. Receiver operating curve (ROC) curve with 1 minus specificity versus sensitivity in 0.01 increments from 0 to 1.

The other metrics of sensitivity, specificity, and accuracy were calculated as

$$\text{Specificity} = TN/TN+FP \quad (4)$$

$$\text{Accuracy} = TP+TN/TP+TN+FP+FN \quad (5)$$

$$\text{Sensitivity} = TP/TP+FN \quad (6)$$

 DOI : 10.35291/2454-9150.2019.0364

TABLE I. Results of the comparison of K = 1 and 2 on all chest CT images (N=16,873). The DSC, MHD, sensitivity, specificity, and accuracy were evaluated and compared. Mean and standard deviation are summarized.

Method		K = 1	K = 2
DSC	*mean*	0.9709	0.7323
	std	0.0511	0.1152
MHD	*mean*	0.5006	1.4270
	std	0.5771	0.5586
Sensitivity	*mean*	0.9585	0.7755
	std	0.0722	0.0697
Specificity	*mean*	0.9981	0.7322
	std	0.0012	0.1329
Accuracy	*mean*	0.9954	0.7321
	std	0.0129	0.1517

IV. CONCLUSION

We have proposed a novel lung contour extraction algorithm capable of detecting juxta-pleural nodules. The algorithm is based on the CV model followed by a Bayesian approach to detect juxta-pleural nodule candidates and eliminate false positives through concave points detection and circle/ellipse Hough transform. In the images that included juxta-pleural nodules, our method exhibited a DSC of 0.9712, MHD of 0.4504, sensitivity of 0.9711, specificity of 0.9637, accuracy of 0.9667, and juxta-pleural nodule detection rate of 96.8%.

REFERENCES

[1] L. Hedlund, R. F. Anderson, P. Goulding, J. Beck, E. Effmann, and C. Putman, "Two methods for isolating the lung area of a CT scan for density information," *Radiology*, vol. 144, no. 2, pp. 353-357, 1982.

[2] R. Uppaluri, T. Mitsa, M. Sonka, E. Hoffman, and G. Mclemman, "Quatification of pulmonary emphysema from lung CT images using texture analysis," *Amer. J. Resp. Crit. Care Med*, vol. 156, no. 1, pp. 248-254, 1997.

[3] I. Amirav, S. S. Kramer, M. M. Grunstein, and E. A. Hoffman, "Assessment of methacholine-induced airway constriction by ultrafast high-resolution computed tomography," *Journal of Applied Physiology*, vol. 75, no. 5, pp. 2239-2250, 1993.

[4] R. H. Brown, C. J. Herold, and C. A. Hirshman, "In Vivo Measurements of Airway Reactivity Using High-Resolution Computed Tomography1, 2," *Am Rev Respir Dis*, vol. 144, pp. 208-212, 1991.

[5] E. A. Hoffman, T. Behrenbeck, P. A. Chevalier, and E. H. Wood, "Estimation of regional pleural surface expansile forces in intact dogs," *Journal of Applied Physiology*, vol. 55, no. 3, pp. 935-948, 1983.

[6] A. M. Boriek, S. Liu, and J. R. Rodarte, "Costal diaphragm curvature in the dog," *Journal of Applied Physiology*, vol. 75, no. 2, pp. 527-533, 1993.

[7] H. A. Gietema, Y. Wang, D. Xu, R. J. van Klaveren, H. de Koning, E. Scholten, J. Verschakelen, G. Kohl, M. Oudkerk, and M. Prokop, "Pulmonary nodules detected at lung cancer screening: interobserver variability of semiautomated volume measurements," *Radiology*, vol. 241, no. 1, pp. 251-257, 2006.

[8] L. Wang and G. Zhang, "Cluster ensemble based image segmentation algorithm," in *2015 Eighth International Conference on Internet Computing for Science and Engineering (ICICSE)*, vol. 00, Nov. 2015, pp. 68–73.

[9] L. Bonanno, S. Marino, A. Bramanti, P. Bramanti, and P. Lanzafame, "Cluster analysis boosted watershed segmentation of neurological image," in *2011 4th International Congress on Image and Signal Processing*, vol. 3, Oct 2011, pp. 1223–1226.

[10] W. Ju, D. Xiang, B. Zhang, L. Wang, I. Kopriva, and X. Chen, "Random walk and graph cut for co-segmentation of lung tumor on pet-ct images," *IEEE Transactions on Image Processing*, vol. 24, no. 12, pp. 5854–5867, Dec 2015.

[11] A. S. Korsager, V. Fortunati, F. van der Lijn, J. Carl, W. Niessen, L. R. stergaard, and T. van Walsum, "The use of atlas registration and graph cuts for prostate segmentation in magnetic resonance images," *Medical physics*, vol. 42, no. 4, p. 16141624, April 2015.

[12] Y. Guo, Y. Gao, and D. Shen, "Deformable mr prostate segmentation via deep feature learning and sparse patch matching," *IEEE Transactions on Medical Imaging*, vol. 35, no. 4, pp. 1077–1089, April 2016.

[13] M. Kallenberg, K. Petersen, M. Nielsen, A. Y. Ng, P. Diao, C. Igel, C. M. Vachon, K. Holland, R. R. Winkel, N. Karssemeijer, and M. Lillholm, "Unsupervised deep learning applied to breast density segmentation and mammographic risk scoring," *IEEE Transactions on Medical Imaging*, vol. 35, no. 5, pp. 1322–1331, May 2016.

[14] J. C. M. Than, N. M. Noor, O. M. Rijal, A. Yunus, and R. M. Kassim, "Lung segmentation for hrct thorax images using radon transform and accumulating pixel width," in *2014 IEEE REGION 10 SYMPOSIUM*, April 2014, pp. 157–161.

[15] A. Mansoor, U. Bagci, Z. Xu, B. Foster, K. N. Olivier, J. M. Elinoff, A. F. Suffredini, J. K. Udupa, and D. J. Mollura, "A generic approach to pathological lung segmentation," *IEEE Transactions on Medical Imaging*, vol. 33, no. 12, pp. 2293–2310, Dec 2014.

[16] Hyoungseop Kim, Seiji Mori, Yoshinori Itai, Seiji Ishikawa, Akiyoshi Yamamoto and Katsumi Nakamura, 2007, Automatic Detection of Ground-Glass Opacity Shadows by Three Characteristics on MDCT Images, World congress on medical physics and biomedical engineering 2006, IFMBE Pro2.

[17] Breiman, L. (2001) Random forests. Machine Learning Journal Paper,45, 5-32.

[18] Wu, X.D. and Kumar, V. (2009) The top ten algorithm in data mining. Chapman & Hall/CRC, London.

[19] Biau, G., Devroye, L. and Lugosi, G. (2008) Consistency of random forests and other averaging classifiers. Journal of Machine Learning Research, 9, 2015-2033.

[20] Jeng-Shyang Pan, Shyi-Ming Chen, Ngoc Thanh Nguyen;November 2010;Computational Collective Intelligence. Technologies and Applications; Taiwan;Springer.

[21] S. G. Armato, G.McLennan, L. Bidautb,et.al"The lung image database consortium(LIDC) and image database resource initiative (IDRI): A completereference database of lung nodules on CT scans," Med. Phys., vol.38,pp.915–931,2011.

 DOI : 10.35291/2454-9150.2019.0364